Ecological Applications, 12(5), 2002, pp. 1528–1547

FUNCTIONAL VARIABILITY OF HABITATS WITHIN THE SACRAMENTO–SAN JOAQUIN DELTA: RESTORATION IMPLICATIONS

LISA V. LUCAS,[1] JAMES E. CLOERN, JANET K. THOMPSON, AND NANCY E. MONSEN

U.S. Geological Survey, 345 Middlefield Road, MS #496, Menlo Park, California 94025 USA

Abstract. We have now entered an era of large-scale attempts to restore ecological functions and biological communities in impaired ecosystems. Our knowledge base of complex ecosystems and interrelated functions is limited, so the outcomes of specific restoration actions are highly uncertain. One approach for exploring that uncertainty and anticipating the range of possible restoration outcomes is comparative study of existing habitats similar to future habitats slated for construction. Here we compare two examples of one habitat type targeted for restoration in the Sacramento–San Joaquin River Delta. We compare one critical ecological function provided by these shallow tidal habitats—production and distribution of phytoplankton biomass as the food supply to pelagic consumers. We measured spatial and short-term temporal variability of phytoplankton biomass and growth rate and quantified the hydrodynamic and biological processes governing that variability. Results show that the production and distribution of phytoplankton biomass can be highly variable within and between nearby habitats of the same type, due to variations in phytoplankton sources, sinks, and transport. Therefore, superficially similar, geographically proximate habitats can function very differently, and that functional variability introduces large uncertainties into the restoration process. Comparative study of existing habitats is one way ecosystem science can elucidate and potentially minimize restoration uncertainties, by identifying processes shaping habitat functionality, including those that can be controlled in the restoration design.

Key words: *benthic grazing;* Corbicula; *hydrodynamics; pelagic consumers; phytoplankton; restoration; San Francisco Bay Delta; shallow water habitat; tidal; zooplankton.*

INTRODUCTION

Environmental science is now driven in part by the search for strategies to reverse or stabilize the impacts of human disturbance, at the scale of ecosystems. Although there is debate about the applicability of the word ''restoration'' (Davis 2000), there is consensus about the need for sustained efforts to rehabilitate, protect, naturalize, or restore biological communities or populations and the ecosystem functions supporting them. This consensus is manifested as growing commitments of public funds and political will to enact restoration plans. Examples in the U.S. include the Estuaries and Clean Waters Act of 2000 (106th U.S. Congress 2000), authorizing federal resources to restore 1×10^6 acres of coastal habitat, and multibillion-dollar programs targeted to rehabilitate populations and ecological functions within the Florida Everglades (Schrope 2001) and California's Sacramento–San Joaquin River Delta (CALFED 2000*a*).

Public investments and political commitments of this magnitude are often based on expectations that restoration actions will result in known outcomes, such as the promotion of specific ecological functions required to sustain target populations. However, the science of ecological forecasting is young (Clark et al. 2001), and our ability to predict responses of ecosystems to manipulation is severely limited (Zedler 2001). Often implicit in restoration expectations is the assumption that particular habitat types provide defined functions and that those functions are provided homogeneously within habitats. In reality, functional attributes can vary in space and time, within and between habitats of the same type, and this functional variability may be amplified when habitats are ''open,'' or subject to the direct influence of neighboring environments (Reiners and Driese 2001). Functional variability within habitat categories makes it difficult to reliably forecast the ecological value of proposed engineered habitats and thus injects uncertainty into the restoration process. The probing of such uncertainty represents a pivotal role for ecosystem science in environmental policy development (Jones 1999).

How can ecosystem scientists probe the uncertainties associated with habitat functional variability? One approach is to compare existing habitats similar to those slated for construction to (1) measure variability in the functions they provide and (2) identify the key processes underlying functional variability. With this critical new information in hand, decision makers can bet-

Manuscript received 15 March 2001; revised 25 September 2001; accepted 30 October 2001; final version received 19 December 2001.

[1] E-mail: llucas@usgs.gov

ter anticipate the range of potential restoration outcomes and develop flexible management strategies accounting for risk (Gunderson 1999). Further, if exploration of variability is focused on underlying processes, including those that are controllable, then the risk associated with predicting outcomes may be minimized (Thomas 1999).

Here we present results of a comparative study designed to measure variability in one ecological function of one aquatic habitat type targeted for restoration in the Sacramento–San Joaquin River Delta, California, USA. This study is a contribution to the CALFED San Francisco Bay–Delta Ecosystem Restoration Program (ERP), conceived to increase populations of threatened and endangered species by creating aquatic, riparian, and upland habitats and by restoring or mimicking the natural processes that sustain those habitats (CALFED 2000*b*). This tidal freshwater ecosystem (hereafter referred to as the ''Delta'') encompasses the complex confluence of California's two largest rivers, the Sacramento and San Joaquin (Fig. 1, top). Ninety-seven percent of the original Delta wetlands and shallow water habitat was diked, drained, and converted for agricultural use, beginning in the late 1800s (Bennett and Moyle 1996). Commitments to large-scale restoration of this ecosystem are motivated by declining abundances of diverse fisheries including migratory species (Chinook salmon, striped bass) and endemic resident species, some of which are threatened or endangered (delta smelt, *Hypomesus transpacificus*; Sacramento splittail, *Pogonichthys macrolepidotus*).

Depressed stocks of diverse fisheries are likely the result of multiple interacting stressors (Bennett and Moyle 1996), one of which is declining productivity in the pelagic food web that provides forage for early feeding stages of endemic fishes. The Delta is an inherently low-productivity ecosystem, with mean annual primary production of only 70 g C/m^2 compared to median estuarine production of 200 g C/m^2 (Jassby et al. 2002). Phytoplankton is the dominant food supply to primary consumers (Jassby and Cloern 2000), but phytoplankton primary production has declined a significant 43% from 1975 to 1995 (Jassby et al. 2002). Parallel declines have been measured in the stocks of mesozooplankton, including rotifers, cladocerans, and native species of copepods, and accumulating evidence suggests that mesozooplankton production is food limited (Kimmerer and Orsi 1996, Müller-Solger et al. 2002). These declines have been most pronounced during summer months, when mean abundances of some zooplankton taxa have declined more than tenfold (Kimmerer and Orsi 1996). Trophic linkages from phytoplankton to mesozooplankton appear to be important for recruitment of threatened species of fishes: all Delta fish that have declined in abundance have pelagic-feeding larval stages (e.g., larval stages of Sacramento splittail feed primarily on cladocerans; Kurth and Nobriga 2001), and some species of concern feed on zooplankton through their entire life history (e.g., copepods are the primary dietary components for delta smelt; Nobriga 1998).

The general coherence in declining primary production, stocks of primary consumers, and multiple species of fishes suggests that recovery of depressed fish stocks could be facilitated by creation of new habitats designed to augment production in pelagic food webs. A specific goal of the CALFED ERP is to create $>$3000 ha of tidal aquatic habitat by breaching dikes around discrete tracts of land. In this study we measured phytoplankton biomass and net production in these habitat types, using two existing tidal lakes as model systems to identify processes that regulate the food-supply function and to determine possible outcomes of this restoration strategy, before large-scale manipulations begin.

Description of the Ecosystem and Comparative Study

The Sacramento–San Joaquin River Delta (Fig. 1, top) is an unusually complex physical system combining attributes of rivers, lakes, and estuaries. Riverine components include deep (up to 15 m) channels with net seaward flows. Lake components include shallow ($\leq$5 m) expanses of open water (e.g., flooded farm tracts) bounded by levees having discrete openings that are pathways for tidally driven water exchanges with adjacent channels (Fig. 1, bottom). Estuarine attributes include tidal fluctuations in water elevation and currents at two time scales: semidiurnal (two flood and ebb tides every 24.84 h) and neap-spring ($\sim$14-d period). This project focused on short-timescale (hours to weeks) processes producing spatial variability in phytoplankton biomass and net growth within and between shallow water habitats. We focused this comparison on summer conditions, with intensive measurements in June because: (1) spring and summer are critical seasons for developing larval fish (Gopalan et al. 1998); (2) June is the month of largest historic primary productivity decline (Jassby et al. 2002); and (3) population declines of cladocerans (*Daphnia* spp. and *Bosmina* spp.) have been most dramatic in summer (Kimmerer and Orsi 1996).

Changes in Delta water quality and biological communities have been carefully documented through monitoring programs sustained over multiple decades. Although these studies have documented well the decline in pelagic primary producers and secondary consumers, little research has been directed to identify or measure the processes of change in the system. Our study design was therefore based on concepts developed from long-term, process-oriented studies of the downstream estuary, San Francisco Bay. Because Delta nutrient (N, P, Si) concentrations are very high (Interagency Ecological Program, *public communica-*

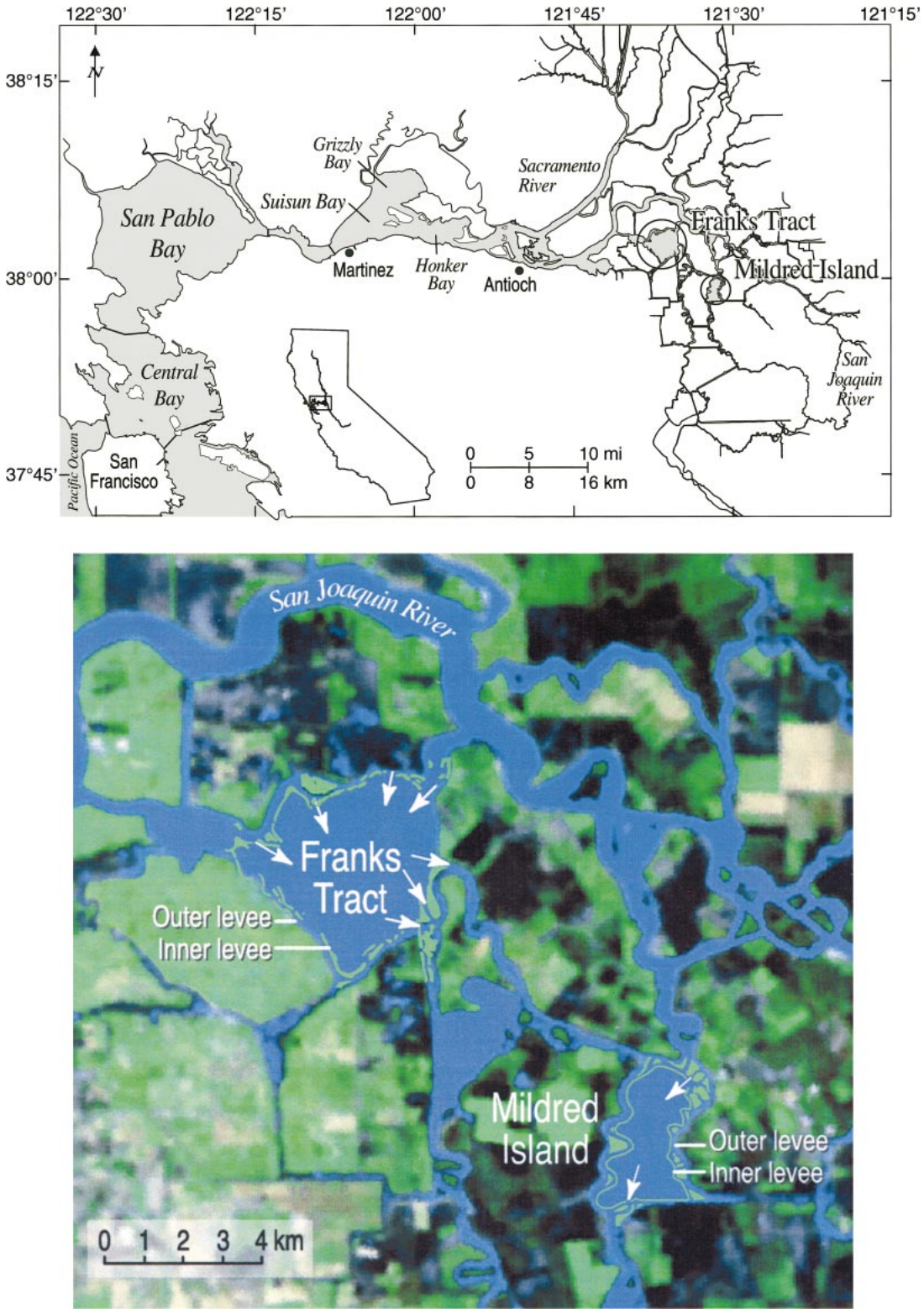

FIG. 1. (Top) Northern San Francisco Bay and the Sacramento–San Joaquin Delta, California, USA. (Bottom) Satellite image of Franks Tract, Mildred Island and surrounding channels, enhanced to show relevant levees. Arrows indicate flow direction during flood tide.

tion),[2] phytoplankton growth rate is a function of water temperature and light availability. Net phytoplankton primary production can be negative in deep habitats where depth-integrated respiration may exceed photosynthesis but positive in shallow habitats where depth-integrated respiration is small (Alpine and Cloern 1988). Further, phytoplankton biomass can be controlled by benthic grazers, especially in shallow regions (Cloern 1982, Lucas et al. 1999*a*, *b*, Thompson 1999). Therefore, phytoplankton growth rate varies along bathymetric gradients between channel and lake domains.

In this study we compared the production and spatial structure of phytoplankton biomass in two flooded farm tracts, Franks Tract (FT) and Mildred Island (MI). These open water habitats have: tidal connections with surrounding river channels (Fig. 1, bottom); maximum tidal currents on the order of 0.1 m/s; mean depth of ~5 m in MI and almost 3 m in FT; and surface areas of 4.1 km^2 for MI and 12.9 km^2 for FT. In each tidal lake we measured changes in phytoplankton biomass and spatial structure over semidiurnal and neap-spring tidal cycles because neap-spring variability in tidal energy regulates phytoplankton dynamics in some estuaries (Cloern 1996). We also quantified the processes that create spatial patchiness: light-limited growth, tidal transport, and grazing. Here we explicitly consider grazing losses to benthic consumers, which are dominated in the Delta by the freshwater clam *Corbicula fluminea* (Hymanson et al. 1994). This species is reported to have substantially reduced phytoplankton biomass in other systems (McMahon 1999). We use the difference between net primary production and benthic consumption as a measure of the residual primary production available to the mesozooplankton, an index of potential secondary production in pelagic food webs.

We chose to focus this comparative study on MI and FT for several reasons. First, FT and MI are geographically close; so, the composition of their source water (primarily San Joaquin River) is similar. Second, unlike recently flooded islands, which may remain in a state of rapid transition, FT (flooded in 1938) and MI (flooded in 1983) are both established regions that may have reached a relative steady state (e.g., with respect to the leaching of dissolved substances from the soil); we have thus attempted to maximize the study of persistent as opposed to transient conditions. Third, creation of new shallow water habitat is proposed near FT and MI (San Francisco Estuary Project 2001); therefore, lessons about ecosystem function in FT and MI are relevant to future similar habitats. Fourth, FT and MI represent a large portion of Delta water volume (Monsen 2001); therefore, ecosystem processes within those sub-environments may have Delta-scale effects.

The current ERP design is based on expectations that creation of new aquatic habitat like FT and MI will enhance sustainability of target species in this ecosystem. However, there is no scientific basis yet for that expectation because there has been no systematic assessment of the biological communities or processes that regulate pelagic production within these habitats. Therefore, this study is an early step of exploratory research to determine if there is a scientific basis for shallow aquatic habitat restoration in this system and to identify processes that may constrain the outcomes of shallow habitat creation as an effective restoration strategy. This short-timescale study offers a detailed ''snapshot'' of MI and FT, whose basic functional characteristics had previously been uninvestigated. The following were previously unknown: presence/absence (MI), spatial distribution (MI and FT), and impact (MI and FT) of benthic grazers; the concentration ranges (MI), spatial variability (MI and FT), short timescale (<1 mo) variability (FT), and long or short timescale variability (MI) of phytoplankton biomass, turbidity, nutrients, and temperature; and the influence of levee breaks and tidally driven transport on water quality (MI and FT).

Methods

Since spatial patchiness of phytoplankton is common in tidal systems, this exploratory study was designed to resolve spatial patterns in phytoplankton biomass and the sources, sinks, and transport processes shaping those patterns. Further, since short timescale processes (hours to weeks) may govern long-term phytoplankton growth and distribution (Lucas et al. 1999*a*, *b*, Lucas and Cloern 2002), this study also resolved neap-spring and intratidal variability. Field measurements yielded time-varying spatial maps of water quality in MI and FT, and numerical models of hydrodynamics and phytoplankton growth were used to study processes and interpret the measured patterns.

Tidal hydrodynamics and particle transport

We used a hydrodynamic numerical model to identify trajectories of passive, conservative particles in FT and MI and to interpret measured spatial patterns of phytoplankton biomass. The DELTA-TRIM model is based on the TRIM3D hydrodynamic code developed by Casulli (1990*a*, *b*, Casulli and Cattani 1994), refined by Gross (1997), and applied to calculate free-surface flows in tidal systems (Cheng et al. 1993, Gross et al. 1999). TRIM3D employs a semi-implicit approach for solving the shallow-water equations with hydrostatic and Boussinesq approximations. Monsen (2001) adapted TRIM3D to the Sacramento–San Joaquin River Delta, and validated computations by comparing calculated time series of stage, flow, and sa-

[2] URL: ⟨http://sarabande.water.ca.gov:8000/~bdtdb/sde8/nutrients11.html⟩

TABLE 1. Dates, locations, and tidal conditions for water quality measurements and benthic sampling was conducted in the Sacramento–San Joaquin Delta, California, USA.

Date	Lake†	Sampling type	Spring/ neap	Tidal phases‡
17 June 1999	MI	water quality mapping	spring	HS, ME, LS
18 June 1999	FT	water quality mapping	spring	HS, ME, LS
22 June 1999	MI	water quality mapping	neap	LS, MF, HS,
23 June 1999	FT	water quality mapping	neap	LS, MF, HS
29 June 1999	MI, FT	benthic	spring	N/A

Note: A total of 12 water quality circuits was completed.
† MI = Mildred Island site; FT = Franks Tract site.
‡ HS and LS represent ''high slack'' and ''low slack,'' respectively; ME and MF represent ''maximum ebb current'' and ''maximum flood current,'' respectively.

linity against measurements for different hydrologic regimes. Calculations presented here were performed using DELTA-TRIM in two-dimensional, depth-averaged mode with a 50-m grid spacing. Major open boundary conditions were specified using measurements of tidal stage and river flow. Model results for FT and MI were extracted from hydrodynamic simulations of the entire Delta (see Fig. 1, top). Simulation results for the field study period (June 1999) were used to describe tidal-scale and residual water circulation and particle transport in FT and MI.

Water quality measurements

We mapped the spatial distribution of phytoplankton biomass (chlorophyll *a*) in FT and MI at different phases of the semidiurnal tidal cycle during a spring tide and a neap tide. A boat followed predetermined sampling circuits while ambient water was pumped to sensors. Total circuit lengths were ~8 km in MI and 16 km in FT, requiring ~1 and 2 h, respectively, to complete. On each of 4 d (17–18 and 22–23 June 1999), we sampled along circuits during two consecutive slack tides and the intervening period of maximum current speed (Table 1). Water was pumped from 0.5 m depth and delivered to instruments for measuring chlorophyll *a* fluorescence (Turner Designs 10-AU fluorometer; Turner Designs, Sunnyvale, California, USA), turbidity (Turner Designs 10-AU fluorometer configured as a nephelometer with a 10-033 nephelometry attachment), and water temperature (Sea-Bird #3-01/F thermistor; Seabird Electronics, Bellevue, Washington, USA). Measurements were recorded every second with a computer, while a global positioning system (GPS) logged boat positions every five seconds. Water quality and GPS data series were synchronized by applying a 5-s median filter to the water quality data. The total number of measurements along each circuit was ~900 for MI and 1500 for FT.

Discrete water samples were collected for determining concentrations of chlorophyll *a*, suspended particulate matter (SPM), and dissolved inorganic nutrients. Aliquots (68.3 mL) were filtered onto GF/F filters (Gelman Sciences, Ann Arbor, Michigan, USA) for chlorophyll *a* and 0.45-μm Nuclepore filters (Whatman, Clifton, New Jersey, USA) for SPM determination. Chlorophyll *a* concentration was determined with EPA Method 445.0 (Arar and Collins 1997), and SPM concentration was measured gravimetrically (Hager 1994). Discrete chlorophyll *a* and SPM concentrations were regressed linearly against the fluorometer and nephelometer voltages, respectively (Fig. 2a–b). Standard errors of the calibration regressions were 0.89 μg/L for chlorophyll *a* and 1.20 mg/L for SPM. We used SPM concentration to estimate the light attenuation coefficient k_t, using an empirical equation (Fig. 2c) determined from historical USGS measurements of k_t with a LI-COR 192S quantum sensor (LI-COR, Lincoln, Nebraska, USA). Residuals around this regression were uncorrelated with chlorophyll *a* ($r^2 = 0.01$), confirming that variability of light attenuation in this turbid environment is caused primarily by variability in suspended sediment concentration. Errors propagated through the voltage–SPM and SPM–k_t relationships resulted in an uncertainty in k_t of 0.09 m^{-1}. Nutrient samples were collected in polyethylene bottles, filtered through 0.45-μm Nuclepore filters, and frozen until analyzed. Concentrations of ammonium, nitrate plus nitrite, dissolved reactive phosphate, and dissolved silica were measured on a Technicon AutoAnalyzer II (APHA 1995).

Benthic sampling and grazing rate

We collected benthic samples on 29 June 1999 to measure biomass of *Corbicula fluminea* (hereafter *Corbicula*) and then estimate its rate of phytoplankton consumption. Grazing rates were based on this single sampling date because *Corbicula* does not grow sufficiently fast to change grazing rates over the timescale of this study (Winternitz 1992). Samples were collected using a 0.05-m^2 van Veen grab (Holme and McIntyre 1971) and sieved through 0.5-mm screen. All *Corbicula* were measured. One complete size range of animals was grouped (1-mm size groups), dried at 60°C, weighed, and then ashed at 500°C to determine ash-free dry mass (AFDM) of each size

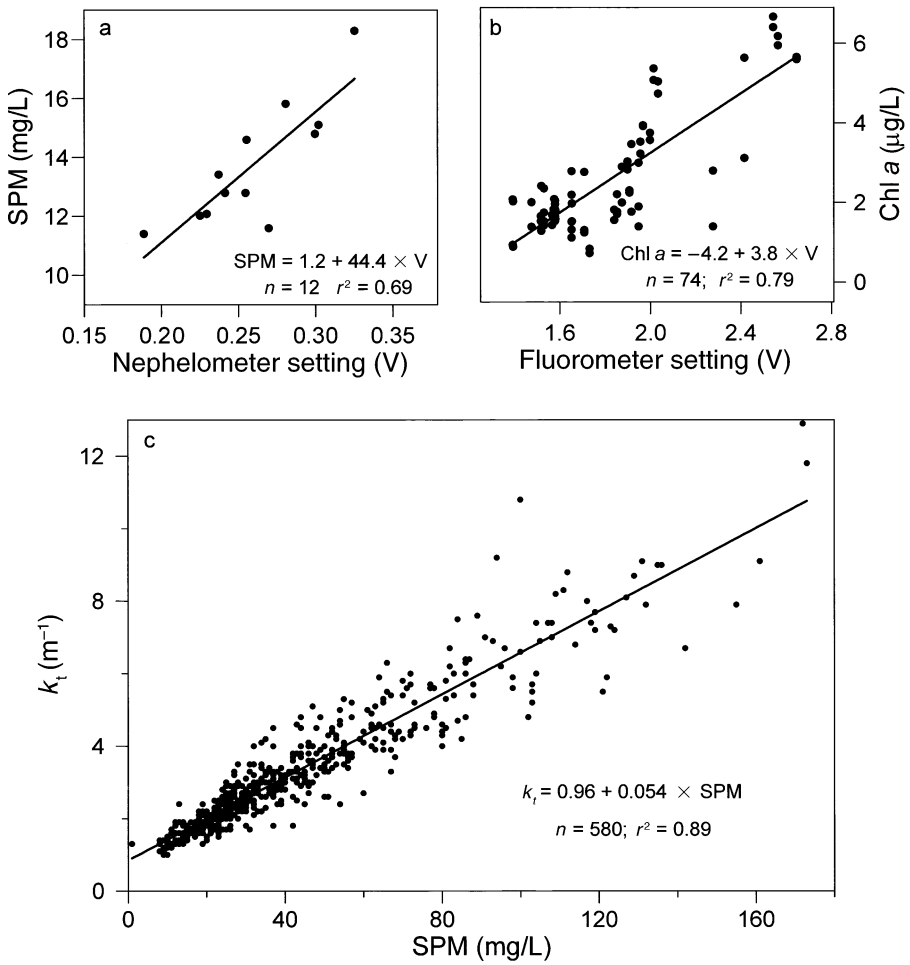

FIG. 2. Calibration of the (a) nephelometer and (b) fluorometer used to measure suspended particulate matter (SPM) and chlorophyll *a* (Chl *a*) concentrations in surface water. (c) Linear regression of light attenuation coefficient k_t against SPM concentration, using 580 measurements in the lower Sacramento River and upper San Francisco Bay between 1977 and 1999 (USGS, *public communication*).[3]

group. Length–mass relationships were then used to calculate dry mass biomass for all samples.

Benthic grazing rate α (in cubic meters per square meter per day) is an effective vertical velocity at the sediment–water interface describing the speed at which a benthic population removes phytoplankton from the water column (Frechette et al. 1989, Koseff et al. 1993, Dame 1996). Pumping rate (in cubic meters per square meter per day) represents the maximum possible grazing rate and applies only when grazing does not reduce near-bed phytoplankton concentrations. However, experiments in the laboratory (Wildish and Kristmanson 1984, Butman et al. 1994, O'Riordan et al. 1995) and field (Frechette and Bourget 1985, Frechette et al. 1989, Dame et al. 1992, Newell and Shumway 1993) have demonstrated that a concentration boundary layer (phytoplankton-depleted zone) may develop over a bed of filter feeders and reduce the amount of phytoplankton ingested if vertical mixing is inadequate. We therefore estimated α from *Corbicula* biomass using the dry mass : pumping rate relationship for *Corbicula* at 20°C (Lauritsen 1986) and O'Riordan et al.'s (1995) correction for a concentration boundary layer. This conservative estimate of benthic grazing rate, reduced for the presence of a concentration boundary layer, was implemented in our estimates of phytoplankton growth discussed below (see *Phytoplankton growth rate*). This approach follows that used previously in studies of the San Francisco Bay (Koseff et al. 1993, Lucas et al. 1998, 1999*a*, *b*).

As an independent check on our grazing rate estimates, we calculated an additional estimate of benthic grazing impact based on *Corbicula* energy requirements. We applied this bioenergetics approach to explore the range of benthic carbon consumption for two

[3] URL: ⟨http://sfbay.wr.usgs.gov/access/wqdata/⟩

TABLE 2. Parameters specified and variables measured or calculated for analyzing phytoplankton sources (light- and temperature-dependent growth), sinks (respiration, benthic grazing), and spatial variability (standard deviation and variogram analysis) in the Franks Tract (FT) site and the Mildred Island (MI) site.

Name	Units	Value/range	Description	Source/comments
Parameters				
a	(mg C·mg chl a^{-1}·h^{-1})/(μmol quanta·m^{-2}·s^{-1})	0.029	photosynthetic efficiency at low irradiance	J. Edmunds (*personal communication*), Edmunds et al. (1999); (1997 measurements near FT and MI)
D	h	15	photoperiod	
$I(0)$	mol quanta·m^{-2}·d^{-1}	59	total daily surface irradiance (quantum flux, photosynthetically active radiation)	CIMIS (California Irrigation Management Information System), *public communication*;† mean June 1999 solar radiation at Davis, California
k_t	m^{-1}	1.7 (MI) 1.8 (FT)	light attenuation coefficient	based on mean measured SPM concentration, June 1999 (this study)
p_{max}	mg C·mg chl a^{-1}·h^{-1}	5.0	maximum instantaneous photosynthetic rate	J. Edmunds (*personal communication*), Edmunds et al. (1999); (1997 measurements near FT and MI)
T	°C	24 (MI) 22.5 (FT)	water temperature	mean measured during June 1999 (this study)
α	m^3·m^{-2}·d^{-1}	0–11	benthic grazing rate	based on benthic samples of *Corbicula*, June 1999 (this study)
Variables				
Chl a	μg/L		phytoplankton biomass concentration measured as chlorophyll a	measured during June 1999 (this study)
[Chl:C]	mg chl a/mg C		phytoplankton cellular ratio of chlorophyll a to carbon	based on approach of Cloern et al. (1995)
h	m		sample separation distance (horizontal variogram axis)	semivariance is calculated for sample pairs that are assigned to a ''class'' of h, where h is the average distance separating sampling points within the class (Robertson 1998)
Δh	m		interval between sample separation distances plotted on a variogram	
H	m		instantaneous water column height	
$I(z)$	μmol quanta·m^{-2}·s^{-1}		instantaneous irradiance at depth z	calculated from exponential decrease of instantaneous surface irradiance with depth (see Cloern et al. 1995)
n_h	—		number of sample pairs separated by distance h	assumes each sample pair is counted twice
$p(z)$	mg C·mg chl a^{-1}·h^{-1}		instantaneous rate of photosynthesis at depth z	see Eq. 5
P	mg C·mg chl a^{-1}·d^{-1}		instantaneous depth-averaged rate of photosynthesis	see Eq. 4
resp	d^{-1}		phytoplankton rate of loss to respiration	see Cloern et al. (1995)
SD	μg chl a/L		standard deviation of phytoplankton biomass measurements along a sampling circuit	
SPM	mg/L		suspended particulate matter concentration	measured during June 1999 (this study)
γ	(μg chl a/L)^2		semivariance (vertical variogram axis)	calculated in this study for chlorophyll a concentration; see Eq. 1
μ_{eff}^{zp}	d^{-1}		effective rate of phytoplankton growth available to pelagic grazers	see Eq. 2
μ_{pel}^{zp}	d^{-1}		pelagic net source of phytoplankton to pelagic grazers	see Eq. 3

† ⟨http://wwwdla.water.ca.gov/cgi-bin/cimis/cimis/data/input_form⟩

TABLE 3. Measured concentration ranges for dissolved nutrients in the Mildred Island (MI) site and the Franks Tract (FT) site, June 1999.

Lake	Range DIN (μmol/L)	Range DRP (μmol/L)	Range DSi (μmol/L)
MI	42.5–56.4	1.6–2.1	216.4–234.0
FT	23.5–31.0	1.5–1.7	200.6–250.5

Note: Abbreviations are as follows: DIN, $NO_3 + NO_2 + NH_4$; DRP, dissolved reactive phosphate; DSi, dissolved silica.

scenarios: (1) bivalve respiration only and (2) moderate rates of growth, respiration, and reproduction. The carbon necessary for maintenance respiration was estimated from the relationships of Foe and Knight (1986) for 20°C (0.56 μL O_2·mg $AFDM^{-1}$·h^{-1}) and 24°C (0.71 μL O_2·mg $AFDM^{-1}$·h^{-1}), which are within the range of temperatures seen during our study. For the growth-reproduction estimate, the range of production was predicted from measured biomass using production : biomass (P:B) ratios of 4 and 5, the range seen in *Corbicula* with moderate growth rates in similar lentic environments (McMahon 1991). Respiration and reproduction for this estimate were then based on the range of measured *Corbicula* assimilation rates (58–71% of consumption is incorporated as biomass; McMahon 1991). The percentage of particles retained after filtration (36–48%) was based on the estimates of Foe and Knight (1986) for temperatures in the range 16–24°C.

Phytoplankton spatial structure

Spatial distributions of chlorophyll *a* are shown as interpolated contour maps based on kriging and a default linear variogram model with zero nugget effect and slope of 1.0. We used two approaches for comparing the spatial variability of chlorophyll *a* along individual circuits: (1) calculating the standard deviation (SD) and (2) variogram analysis. The standard deviation provides a bulk measure of chlorophyll *a* variability along a sampling circuit (i.e., at a particular tidal phase) without spatial information. Variograms display the semivariance γ, a measure of sample dissimilarity, as a function of sample separation distance

$$\gamma(h) = \frac{1}{2n_h} \sum_{i=1}^{n_h} \left[f(\mathbf{p}_i) - f(\mathbf{q}_i) \right]^2 \quad (1)$$

where n_h is the number of data pairs separated by distance h, f is chlorophyll *a* concentration, and $\mathbf{p}$ and $\mathbf{q}$ are vector sample locations such that $\|\mathbf{p}_i - \mathbf{q}_i\| = h$. Semivariance usually increases from near zero for $h = 0$ to larger values for greater separation distances, across which data values are less similar. A variogram may plateau for large h, indicating that paired measurements are practically uncorrelated (Isaaks and Srivastava 1989, Kitinidis 1997). If a variogram continues to rise with increasing separation distance, then a ''trend'' (spatially variable mean) may be present (Kitinidis 1997).

A trend was present in some of the MI chlorophyll *a* transects; since we are interested in all influences on chlorophyll *a* distribution, we did not remove trends from the data. Variograms are sensitive to choices of the analyst (e.g., the chosen interval[s], Δh, between separation distances plotted on a variogram), so we used a fixed method of variogram generation for all cases. We calculated variograms using a variable Δh so that higher resolution could be applied near the origin (Kitinidis 1997). Best-fit isotropic variogram models were produced for each case so that spatial structure for different lakes and tidal conditions could be compared quantitatively.

Phytoplankton growth rate

We used the effective rate of phytoplankton growth available to pelagic grazers, μ_{eff}^{zp}, as a metric for comparing the food-supply functions of MI and FT. At a point in space, μ_{eff}^{zp} is the depth-average of local sources and sinks of phytoplankton biomass (light-dependent photosynthesis, respiration, benthic grazing), assuming the water column is vertically well mixed (Lucas et al. 1999*a*). Zooplankton grazing was not included because the objective was to measure the supply rate of phytoplankton biomass *to* pelagic grazers. Positive μ_{eff}^{zp} indicates that the coupled benthic–pelagic system functions as a local net source of phytoplankton biomass to pelagic grazers; negative μ_{eff}^{zp} occurs when the local system is a net phytoplankton sink.

We used a depth-averaged numerical model of phytoplankton growth to calculate μ_{eff}^{zp} from incident sunlight (photosynthetically active quantum flux), tidally oscillating water column height (H), benthic grazing rate (α), water temperature (T), and light attenuation coefficient (k_t). Since μ_{eff}^{zp} varies continuously in time due to tidal oscillations of H, the diurnal light cycle, and their relative phasing, we do not report instantaneous values of calculated μ_{eff}^{zp}; instead, we report values of μ_{eff}^{zp} for which the effects of these short-term fluctuations have been averaged out. (In a separate study, Lucas and Cloern [2002] have shown that spring-neap variability in net phytoplankton growth rates should not be significant in this system, due to the relatively small tidal range [~1 m].) Parameters used to calculate μ_{eff}^{zp} are based on measurements from June 1999 where possible and, otherwise, on previous studies in the Sacramento–San Joaquin River Delta (see Table 2).

A general expression for μ_{eff}^{zp} (Lucas et al. 1999*a*) is

$$\mu_{eff}^{zp} = \mu_{pel}^{zp} - \frac{\alpha}{H} \quad (2)$$

where μ_{pel}^{zp} includes pelagic processes (carbon assimilation, chlorophyll synthesis, respiration), and $-\alpha/H$ is benthic grazing loss.

The phytoplankton source μ_{pel}^{zp} was calculated using

$$\mu_{pel}^{zp} = P \times [\text{chl:C}] - \text{resp} \quad (3)$$

where P is the depth-averaged photosynthetic carbon assimilation rate per unit of chlorophyll a; [chl:C] is the ratio of chlorophyll a to carbon in phytoplankton; and resp is respiration loss rate. P is based on the depth integral of the photosynthesis–irradiance function

$$P = \frac{1}{H}\int_{-H}^{0} p(z)\, dz \quad (4)$$

where

$$p(z) = p_{max}[1 - \exp(-I(z)a/p_{max})] \quad (5)$$

Eq. 5 describes instantaneous photosynthesis p at depth z as a function of light $I(z)$ (determined by solar radiation at the water surface $I[0]$, photoperiod D, and attenuation coefficient k_t; Cloern et al. 1995) and physiological parameters a and p_{max}. P was calculated by integrating Eq. 5 with a series approximation similar to that of Platt et al. (1991). The [chl:C] ratio and respiration rate were calculated using the approach of Cloern et al. (1995), which describes an adaptive rate of chlorophyll synthesis depending on temperature, light, and nutrient availability. Here, we assume that nutrients are not limiting (see Table 3). We tested the sensitivity of μ_{pel}^{zp} to error in k_t and found resultant error in μ_{pel}^{zp} to be <0.03 d^{-1}, or $<4\%$.

Results

Model simulations of tidal hydrodynamics and particle transport

Using a model simulation of tidal hydrodynamics for the field study period (June 1999), several numerical particle tracking experiments were performed for identifying important transport processes in MI and FT and interpreting June 1999 water quality measurements. Here we present three specific particle release scenarios demonstrating transport processes that appear to be critical in shaping observed water quality patterns. (See Appendix for animated model results.)

Interaction of MI interior with northern channel.—Simulated particle tracks (Fig. 3) show tidal-scale transport between the interior of MI and a neighboring channel. For this simulation, we initialized passive numerical particles in the river channel northeast of MI during low slack tide (Fig. 3a). During the subsequent flood tide, many of those particles were carried into northern MI (Fig. 3b). During the following ebb tide (Fig. 3c), the majority of these particles were transported back into the northeast or northwest channel. Two tidal cycles after particle release, several particles remained inside MI (Fig. 3d).

Longer residence time in southern MI.—Passive particles were also initialized uniformly inside MI during high slack tide (Fig. 4a). Water mass and particles in southern MI exchanged with the southern channel, as channel-to-lake transport during ebb tide and lake-to-channel transport during flood (see Fig. 1, bottom, and Fig. 4c). Because the southern opening is smaller and shallower than the NE opening, the rate of mass and momentum exchange with the southern channel was less than with the northern channels. As a result, particle flushing was more efficient in northern MI and, after 10 complete tidal cycles (Fig. 4d), a spatial gradient in particle density (increasing to the south) was evident. In model animations (see Appendix), we observed another important feature of this simulation: that particle tidal excursion (an indicator of dispersion and flushing) generally decreased southward and appeared to reach a minimum in the southeast portion of MI, probably due to the isolation of that region from significant levee breaks (L. V. Lucas and N. E. Monsen, *personal observation*).

Interaction of FT with outer channels.—Model-derived particle tracks in Fig. 5 demonstrate channel-lake interaction in eastern FT. We initialized passive particles in the southeast river channels outside FT during high slack tide (Fig. 5a). During ebb, the majority of the particles entered FT, some traversing approximately one-third of the lake during one half tide cycle (Fig. 5b). During the following flood, many particles returned to the channels while others remained in the

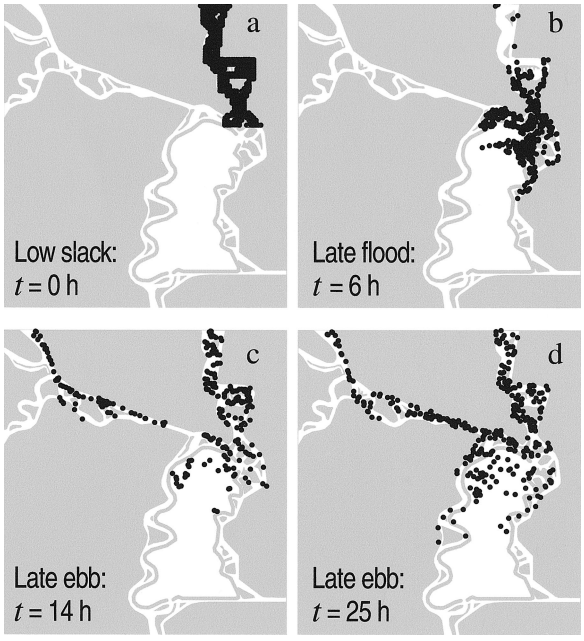

FIG. 3. Locations of passive numerical particles (black dots) showing tidal interaction of northern Mildred Island with channels. Particle tracks were calculated by the DELTA-TRIM hydrodynamic model for June 1999 conditions (Monsen 2001). Gray represents land (including levees); white represents water. Particles were initialized in the northern channel (a) and then tidally sloshed between the lake interior and adjacent channels (b, c). In the longer term, net import of river-borne particles to the lake, as well as substantial dispersion, occurred (d).

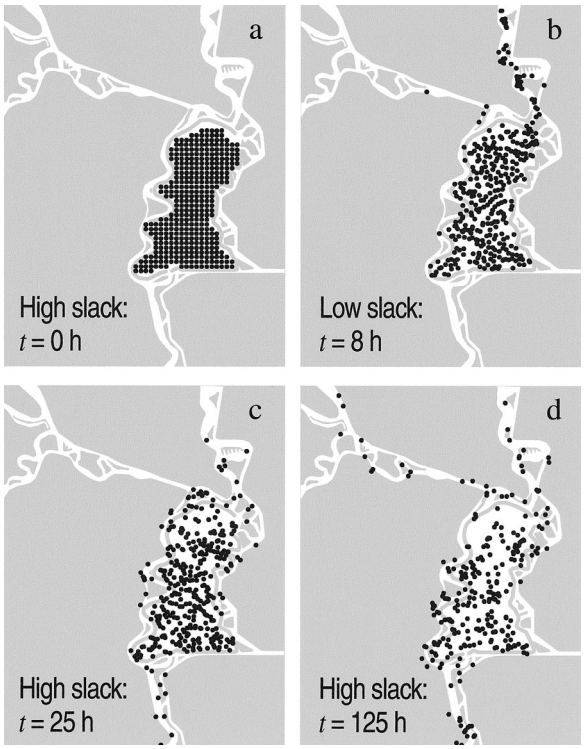

FIG. 4. Locations of passive numerical particles (black dots) showing increased retention of particles toward the south in the Mildred Island (MI) site. Particle tracks were calculated by the DELTA-TRIM hydrodynamic model for June 1999 conditions (Monsen 2001). Gray represents land (including levees); white represents water. Particles were initialized uniformly throughout the lake interior (a) and then tidally sloshed between the lake interior and adjacent channels (b, c). In the long term, a north–south gradient in particle density developed (increasing to the south), suggesting longer residence times in southern MI (d).

lake near the eastern boundary (Fig. 5c). After eight full tide cycles (Fig. 5d), channel-born particles had infiltrated the eastern half of the lake, representing long-term net transport into the lake. Similar tidal-scale interaction between neighboring channels and the lake interior also occurs at several northern openings (see Fig. 1, bottom), increasing the potential for residual (tidally averaged) import of channel-derived particles to the lake.

Spatial variability of phytoplankton biomass

Chlorophyll *a* concentrations in MI ranged from ~1 to 10 μg/L, with individual circuit averages of ~3.5 μg/L. In FT, chlorophyll *a* ranged from 0.4 to almost 6 μg/L, with circuit averages of 1–2 μg/L. In MI (Fig. 6), chlorophyll *a* generally increased southward, reaching maximum concentrations in the southeast part of the lake and minima in the northern portion. Maximum chlorophyll *a* concentrations in MI were highest (10.0 μg/L) during neap tide and lowest (7.8 μg/L) during spring tide. The standard deviation (SD) of chlorophyll *a* in MI was highest during neap tide and during high slack. In FT (Fig. 7), chlorophyll *a* generally increased slightly toward the east, and maximum concentrations were 6.0 μg/L during neap tide compared to 5.0 μg/L during spring tide. The SD of chlorophyll *a* concentration in FT was highest during neap tide and during low slack. In most cases the SD of chlorophyll *a* in FT was less than half the corresponding SD of chlorophyll *a* in MI.

Variograms were produced from chlorophyll *a* concentrations along each transect (Fig. 8). Most of these variograms do not clearly plateau for the length scales of interest; therefore, a trend may be present in the data. For this reason, we compared the semivariance γ at a particular sample separation distance, $h = 1500$ m. We chose this particular value of h because: (1) for a nonstationary function (i.e., a function containing a trend, like some in Fig. 8), γ may be unreliable for h larger than half the maximum sample separation distance (Kitinidis 1997); and (2) variograms from all sampling circuits were well resolved at $h \approx 1500$ m. We calculated γ_{1500} by substituting $h = 1500$ m into the best-fit variogram model for each case, and we used γ_{1500} (shown in Fig. 8) to compare spatial structures of phytoplankton biomass between lakes and tidal conditions. Large γ_{1500} indicates that samples separated by 1500 m are dissimilar and reflects sharp spatial gradients in chlorophyll *a* concentration, whereas small γ_{1500} suggests weak spatial gradients. In MI, γ_{1500} was consistently highest at high slack and during neap tide.

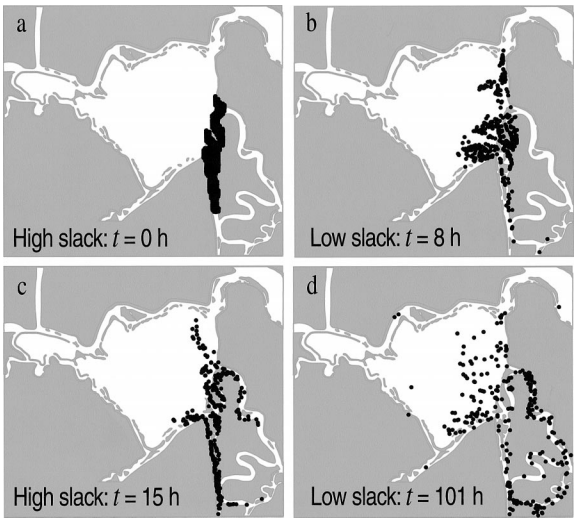

FIG. 5. Locations of passive numerical particles (black dots) showing tidal interaction of eastern Franks Tract with southeast channels. Particle tracks were calculated by the DELTA-TRIM hydrodynamic model for June 1999 conditions (Monsen 2001). Gray represents land (including levees); white represents water. Particles were initialized in the southeast channels (a) and then tidally sloshed between the lake interior and adjacent channels (b, c). In the long term, net import of river-borne particles to the lake, as well as substantial dispersion, occurred (d).

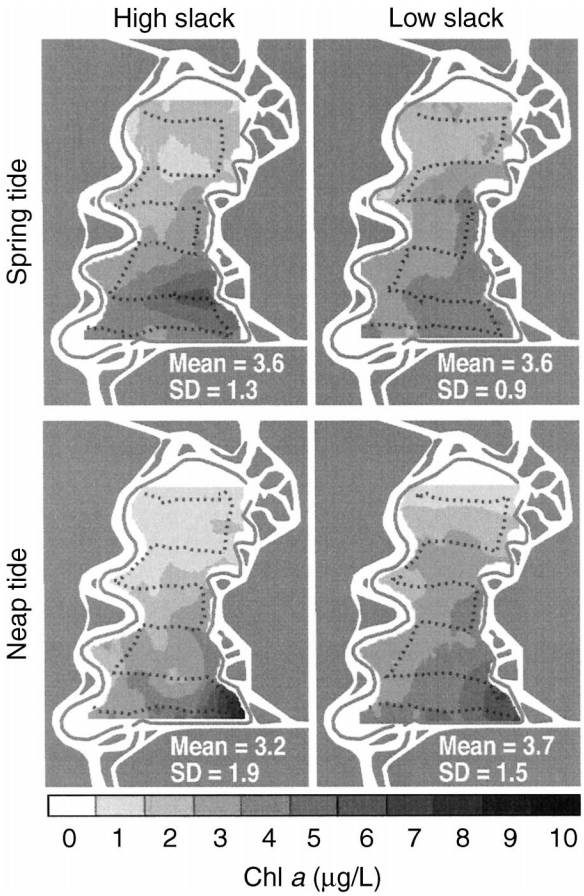

FIG. 6. Interpolated chlorophyll *a* (Chl *a*) contours for Mildred Island, June 1999. Overlaid on the chlorophyll *a* contours are the boat tracks (dotted lines) from which the contours were generated. Mean and SD were calculated for measured chlorophyll *a* along the boat tracks.

In FT, γ_{1500} was consistently highest at low slack and during neap tide. γ_{1500} was an order of magnitude larger in MI than in FT.

Additional water quality measurements

SPM concentrations were less variable than chlorophyll *a*. In MI, the range of SPM concentrations from all sampling circuits was 11–18 mg/L, with a mean of ~13 mg/L during both spring and neap tide. In FT, SPM concentrations ranged from 10 to 25 mg/L, with a mean of ~15 mg/L. Water temperature ranged from 23°–25°C in MI and from 21°–24°C in FT. Dissolved inorganic nitrogen concentrations were uniformly high, with all measurements exceeding 40 μmol/L in MI and 20 μmol/L in FT (Table 3). Concentrations of dissolved reactive phosphorus and dissolved silica were also well above concentrations that limit phytoplankton growth (Table 3). The nutrient and chlorophyll *a* concentration ranges measured in this spatially intensive study were generally similar to those measured in a complementary study in which discrete samples were collected in MI and FT approximately seasonally, from autumn 1998 through summer 2000 (W. Sobczak, *personal communication*).

Benthic grazing rates

Benthic grazing rates were spatially variable within and between the lakes. At most sampling stations in MI (Fig. 9a), *Corbicula* was absent, so calculated benthic grazing rates were zero. *Corbicula* was present ($\alpha > 0$) at about half the sites in northern MI but only one site in the south. There was no clear spatial trend in α within the northern half of MI. Overall, α ranged from 0 to 3 $m^3 \cdot m^{-2} \cdot d^{-1}$ and averaged 0.4 $m^3 \cdot m^{-2} \cdot d^{-1}$ in MI. *Corbicula* was abundant throughout FT, where calculated $\alpha > 0$ at all interior sites (Fig. 9b), ranging from 1 to 11 $m^3 \cdot m^{-2} \cdot d^{-1}$. This grazing rate range corresponds to 60 *Corbicula*/m^2 (= 113 g AFDM/m^2) for $\alpha = 1$ $m^3 \cdot m^{-2} \cdot d^{-1}$ and 2100 *Corbicula*/m^2 (= 2174 g AFDM/m^2) for $\alpha = 11$ $m^3 \cdot m^{-2} \cdot d^{-1}$. The mean estimated benthic grazing rate in FT was 4.4 $m^3 \cdot m^{-2} \cdot d^{-1}$, an order of magnitude greater than in MI. The abundance of *Corbicula* reported for FT is representative of its abundance in this sub-environment, as shown by the similarity between our abundance data and summer abundances measured by the California Department of Water Resources at one station in FT from 1977 to 1995 (In-

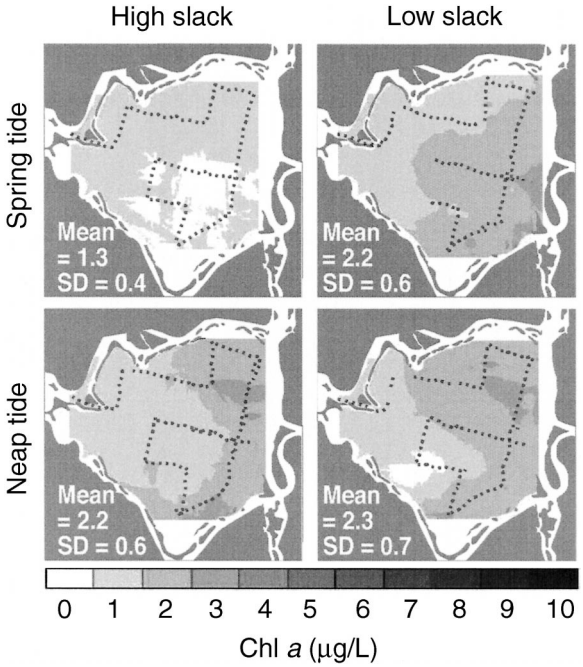

FIG. 7. Interpolated chlorophyll *a* (Chl *a*) contours for Franks Tract, June 1999. Overlaid on the chlorophyll *a* contours are the boat tracks (dotted lines) from which the contours were generated. Mean and SD were calculated for measured chlorophyll *a* along the boat tracks.

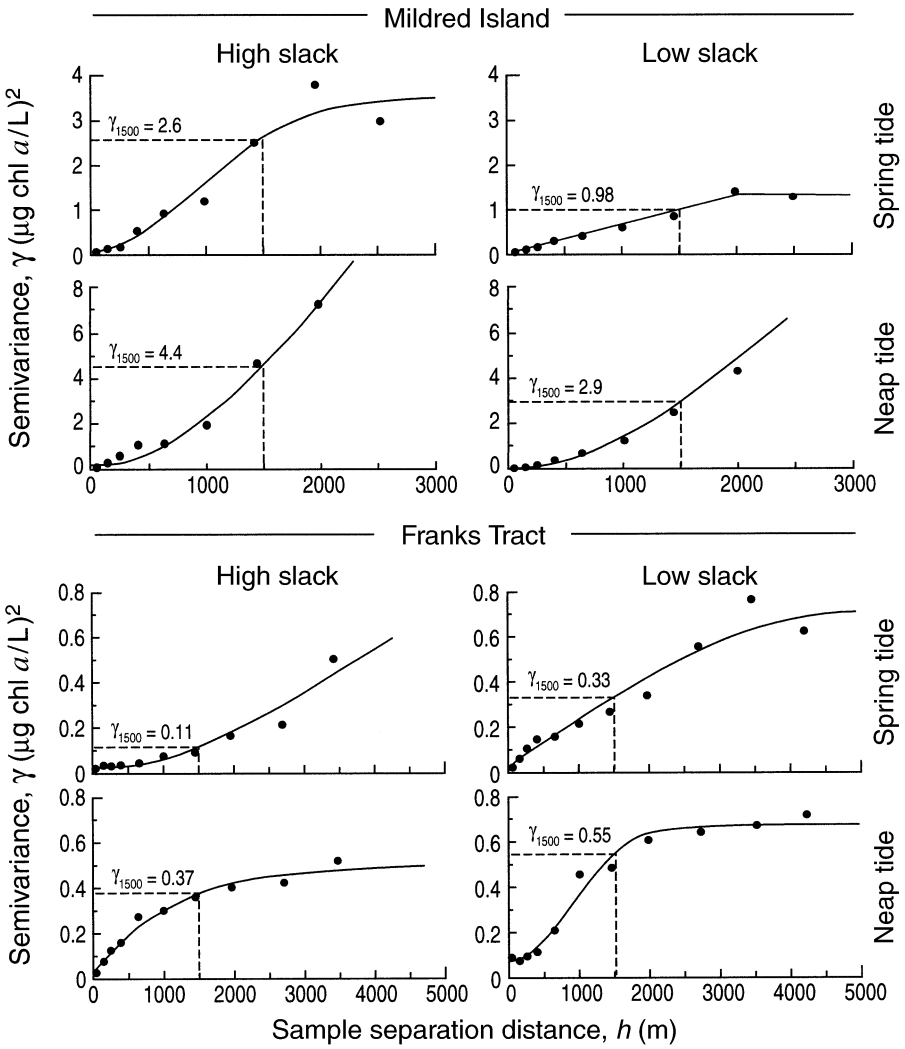

FIG. 8. Variograms generated from chlorophyll *a* measurements in Mildred Island and Franks Tract. Vertical axes are semivariance, γ, and horizontal axes are sample separation distance, *h*. Dots represent experimental variogram calculated from measurements; curves represent best-fit variogram models for each case. γ_{1500}, the semivariance for $h = 1500$ m, was calculated from the variogram model for each case and is indicated on each variogram.

teragency Ecological Program for the Sacramento–San Joaquin Estuary, *public communication*).[4]

We compare the range of estimated phytoplankton carbon consumed by the *Corbicula* (lake-averaged α multiplied by phytoplankton biomass as carbon) with the range of estimated carbon required for maintenance respiration and moderate rates of growth and reproduction (Table 4). The low end of the grazing-based range (40 and 320 kg C·km^{-2}·d^{-1}, respectively, for MI and FT) accounts for the effects of a concentration boundary layer and so is considered the best estimate within that range. For the energetics-based method, values at the low end of the growth-reproduction range (50 and 350 kg C·km^{-2}·d^{-1}, respectively, for MI and FT) are likely to be the best estimate of *Corbicula* carbon intake, due to food limitation (Foe and Knight 1985). For both lakes, the best estimates of benthic carbon consumption for the two approaches are very similar, lending confidence in the benthic grazing rates used below in our calculations of net phytoplankton biomass available to pelagic grazers ($\mu_{\text{eff}}^{\text{zp}}$).

We did not collect benthic samples in the channel outside MI in June 1999; however, from a sample collected during October 1998 in the channel northeast of MI (A. R. Stewart, *personal communication*, not shown in Fig. 9), the estimated α was an astounding 19 m^3·m^{-2}·d^{-1}.

Phytoplankton production for pelagic grazers

The effective phytoplankton growth rate, $\mu_{\text{eff}}^{\text{zp}}$, was ≥ 0 at all sites in MI and, in most cases, positive; the

[4] URL: ⟨http://www.iep.ca.gov/wqdata/disc_water/⟩

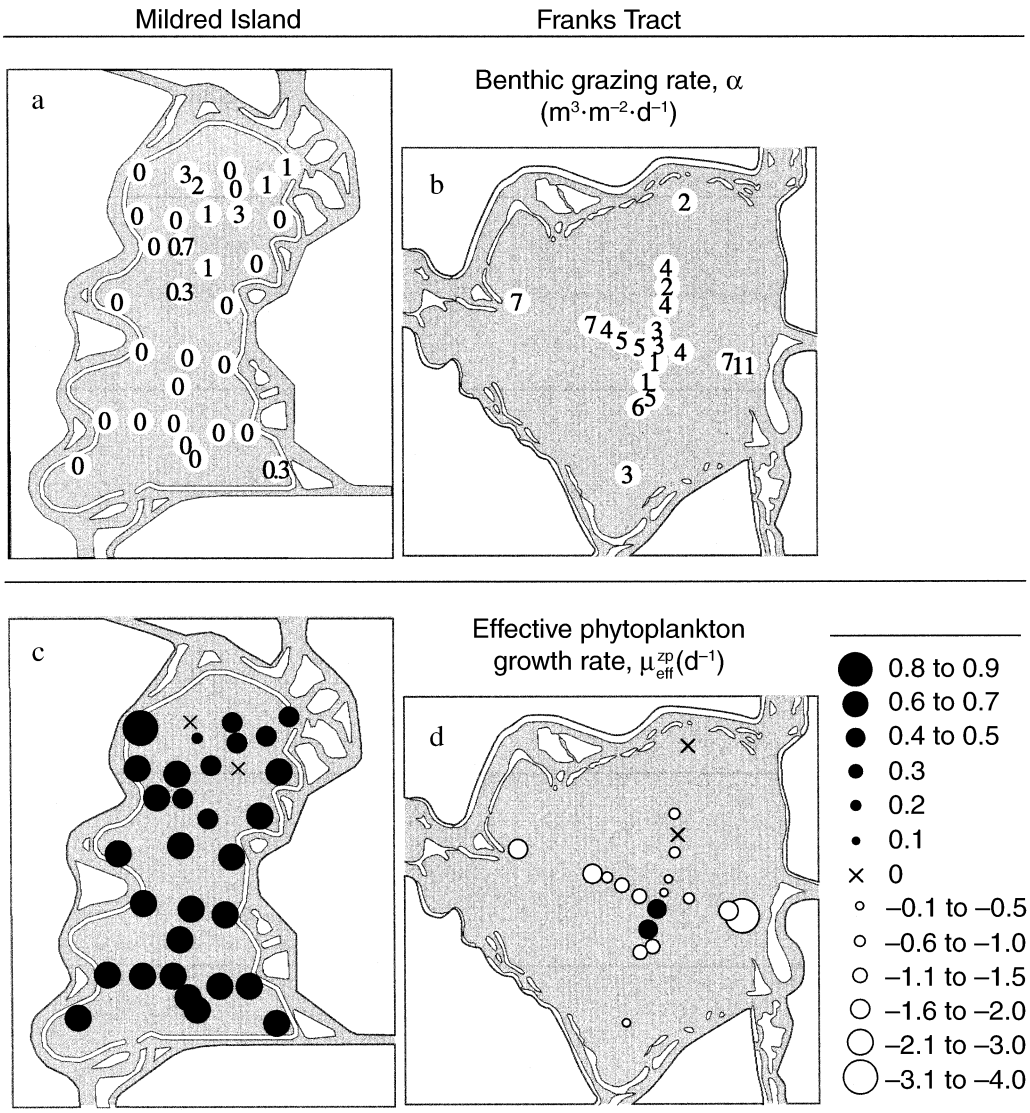

FIG. 9. Top: Benthic grazing rates calculated from measured size, density, and biomass of *Corbicula* at sampling sites in (a) Mildred Island and (b) Franks Tract on 29 June 1999. Bottom: Calculated μ_{eff}^{zp}, the effective rate of phytoplankton growth available to pelagic grazers, for (c) Mildred Island and (d) Franks Tract in June 1999. Solid black circles indicate positive values (photosynthesis > respiration + benthic grazing); empty circles indicate negative values (photosynthesis < respiration + benthic grazing); ''×'' indicates a balance between photosynthesis, respiration, and benthic grazing.

range in MI was 0–0.8 d^{-1} (Fig. 9c), with a mean of +0.5 d^{-1}. In contrast, μ_{eff}^{zp} inside FT was negative in most cases; the range in FT was −3.3 to +0.4 d^{-1} (Fig. 9d), with a mean of −0.9 d^{-1}. We used mean measured phytoplankton biomass, *H*, and calculated μ_{eff}^{zp} and [chl:C] to estimate overall rates of phytoplankton production during our June 1999 study: MI *produced* a net 900 kg/d of phytoplankton carbon for pelagic grazers, and FT *consumed* a net 2300 kg C/d (respiration and benthic grazing losses exceeded photosynthesis).

DISCUSSION

Phytoplankton spatial variability

Spatial variability of phytoplankton biomass within and between MI and FT was significant in June 1999. Within each lake, chlorophyll *a* concentrations varied by a factor of ~10. Maximum and mean chlorophyll *a* concentrations in MI were approximately twice those in FT (Figs. 6–7). Within MI, a strong north-south chlorophyll *a* gradient was consistently observed; in FT, a weaker west-east gradient was usually apparent. Higher

TABLE 4. Estimated June 1999 phytoplankton carbon consumption by *Corbicula* (''grazing-based'' estimate) and *Corbicula* carbon requirement (''energetics-based'' estimate) for the Mildred Island (MI) site and the Franks Tract (FT) site.

Lake	Estimated phytoplankton carbon consumed by *Corbicula* (kg C·km^{-2}·d^{-1})	Estimated *Corbicula* carbon requirement (kg C·km^{-2}·d^{-1})	
		Maintenance respiration	Moderate growth and reproduction
MI	**40**–50	6–7	**50**–90
FT	**320**–370	40–50	**350**–590

Note: Values in bold represent our best estimate of *Corbicula* carbon intake for each lake and each method.

SD in MI indicates greater spread about the mean concentration than in FT, and larger γ_{1500} in MI suggests sharper spatial gradients than in FT. Two sets of processes interact to generate these patterns of spatial variability: (1) hydrodynamics and (2) spatially variable sources and sinks. Here, we discuss each set of processes in detail.

Hydrodynamic processes.—Our hydrodynamic simulations taught us several lessons on how tidal transport can strongly shape the spatial structure of phytoplankton biomass. First, interaction between the lakes and their neighboring channels is significant at tidal timescales. For example, northern MI receives water and particles from the northeast river channel during flood tide, and many of those particles return to the channel during ebb (Fig. 3). Similarly, eastern FT receives water and particles from the southeast river channels during ebb tide, and some of those particles leave FT during flood (Fig. 5). Phytoplankton cells are living particles, with growth kinetics dependent on local conditions (e.g., light and grazing), so they are influenced by the total range of conditions experienced along their tidal trajectories. Therefore, water and phytoplankton sampled inside tidal lakes may be of recent riverine origin and not necessarily or solely characteristic of the conditions at the sampling location.

Second, residual import of river water can be significant: simulated riverine particles remained inside MI (Fig. 3) and FT (Fig. 5) after an integer number of flood/ebb cycles. Let us extend our conceptualization of discrete ''particles'' to continuous ''concentration fields.'' An input of riverine water to a lake will always mix to some extent with the resident lake water. The two water types will irreversibly dilute each other and collectively create a blob of combination river-lake water, whose perimeter bounds the extent of intruding river water and whose volume is larger than the original riverine slug. Unless the blob of river-influenced water leaves the lake completely and permanently during the next half tide cycle (impossible with symmetric tides, due to diffusion, and unlikely with real tides), some amount of river water is left behind (net import from the river to the lake), just as there is usually net export of some lake water to the river. The combination of tidal advection and mixing/dilution therefore diffuses the lake-channel concentration gradient. Our numerical particle tracks suggest that river-to-lake import at FT and MI may consist of more than mild diffusion, since numerous particles were left behind in each lake after an integer number of flood/ebb cycles.

Third, interaction of tidal transport with complex geometry can rapidly disperse a particle cloud, like a plankton patch (Fig. 3). Geometric features including levees, islands, channel bends, and channel junctions generate transport asymmetries by providing multiple flow routes and producing horizontal variations in water momentum and tidal phase (J. Burau and M. Stacey, *personal communication*). Combined with oscillatory tidal transport, these features can efficiently disperse a scalar patch (e.g., compare the compact particle cloud in Fig. 3a with the dispersed cloud in Fig. 3c–d).

Fourth, geometry and hydrodynamic forcing combine to produce circulation patterns in tidal lakes that create distinct zones of slow exchange where mass can accumulate. Shear-induced dispersion is generally greatest where and when water moves most rapidly, so dispersion is more pronounced in high-speed areas than in regions where water moves slowly. Similarly, strong spring-tide currents generate more shear-induced dispersion than neap-tide currents. In MI, tidal mixing and particle flushing decrease southward (Fig. 4), with current velocities and dispersion reaching apparent minima in the southeast; this region appears to be a hydrodynamic ''dead zone'' where water and particles recirculate to maintain persistent high phytoplankton biomass (Fig. 6). These model-based findings are consistent with the observations of Cuetara and Burau (USGS, *public communication*),[5] whose drifter experiments showed increased tidal excursion and dispersion in northern MI (relative to southern MI) and during spring tide (relative to neap tide).

Phytoplankton sources and sinks.—We have used $\mu_{\text{eff}}^{\text{zp}}$ to encapsulate local sources and sinks of phytoplankton biomass and to represent an environment's inherent capacity to fuel pelagic secondary production. This ecosystem function can vary substantially between shallow tidal habitats (Fig. 9c–d), and the overriding factor in that variability can be the strength of the benthic sink for phytoplankton biomass (Fig. 9a–b). In June 1999, FT was densely inhabited by *Corbicula*, but this filter feeder was less abundant in MI. In FT, $\mu_{\text{eff}}^{\text{zp}}$ was predominantly negative because the combined benthic grazing and respiration sinks exceeded the algal growth rate (Fig. 9d); in MI $\mu_{\text{eff}}^{\text{zp}}$ was ≥ 0 everywhere, indicating that phytoplankton growth rate exceeded respiration and benthic grazing, leaving a large residual phytoplankton production available to pelagic grazers (Fig. 9c). Therefore, these two tidal lakes functioned in opposite ways: MI was a net source

[5] URL: ⟨http://sfbay.wr.usgs.gov/access/flow/drifterstudies/⟩

of phytoplankton biomass to the pelagic food web, and FT was a net sink. This field-based finding is consistent with the model-based hypothesis of Lucas et al. (1999*a*) that shallow waters can function as either sources *or* sinks of phytoplankton biomass.

Together, transport and spatially variable phytoplankton sources and sinks produce patterns in chlorophyll *a*. Next we discuss both classes of processes and their coupled effects on observations of phytoplankton biomass.

Tidal sloshing and dispersion explain high growth rate, low biomass.—Oscillatory tidal transport (''tidal sloshing'') between sub-environments with different growth and consumption rates can influence phytoplankton biomass at a point in space (Lucas et al. 1999*b*). Our hydrodynamic model showed tidal-scale sloshing of particles between northern MI and the outside river channel (Fig. 3). This is important because phytoplankton growth environments inside and outside MI were different: $\mu_{\text{eff}}^{\text{zp}}$ in the deep channel was smaller than inside MI because of the channel's lower depth-averaged irradiance. If benthic grazing occurred in the channel (likely, based on the measurement of A. R. Stewart, *personal communication*), then $\mu_{\text{eff}}^{\text{zp}}$ in the channel was smaller yet and probably negative. Water and phytoplankton sloshed between these distinct growth habitats over hourly time scales. Chlorophyll *a* concentrations in northern MI were consistently low relative to southern MI and similar to concentrations in the outside channel (generally ~1–3 μg/L). A comparison of chlorophyll *a* distributions during high and low slack (Fig. 6) shows a low-chlorophyll *a* zone expanding southward during flood tide, causing chlorophyll *a* concentrations at any one location to change over scales of hours. The lower concentrations in the north resulted partly from repeated tidal excursions of water and phytoplankton into the channel where phytoplankton growth rates were small or negative. Dispersion of low-chlorophyll *a* river water into MI, combined with higher *Corbicula* densities in northern MI than in southern MI (Fig. 9a), also contributed to low chlorophyll *a* concentrations in northern MI.

Spatially variable residence time contributes to patchiness.—Spatial structure of phytoplankton biomass can be controlled by spatially variable export rate or, inversely, residence time (Lucas et al. 1999*b*). Hydrodynamic model results (Fig. 4) show that water masses were retained in southern MI over time scales longer than the phytoplankton doubling time (~1 d), allowing biomass accumulation and high concentrations such as those measured in June 1999 (Fig. 6). This effect was maximized in southeast MI, where tidal excursions and particle flushing appeared to be smallest. Thus, MI was characterized by a northern region having vigorous tidal exchange with less productive outside channels, and a southern region characterized by high local growth rates and relatively long water retention times, with water movement most sluggish in the southeast. These physical characteristics, combined with a weak north-south gradient in $\mu_{\text{eff}}^{\text{zp}}$, produced the strong longitudinal gradient of phytoplankton biomass.

Import offsets negative effective growth rates.—Tidally averaged import can deliver phytoplankton biomass to regions where the net phytoplankton growth rate is negative (Lucas et al. 1999*b*). This may explain how phytoplankton biomass was sustained in FT (Fig. 7), where $\mu_{\text{eff}}^{\text{zp}}$ was predominantly negative (Fig. 9d). Several levee breaks provide exchange routes between the interior of FT and its neighboring channels (Fig. 1b), rendering FT much ''leakier'' than MI. Hydrodynamic modeling shows that tides introduce water and particles from neighboring channels (Fig. 5) to inner FT and that some of those particles may not leave during subsequent tide cycles. Chlorophyll *a* concentrations in channels bounding FT generally ranged from 1 to 3 μg/L. Given this range of chlorophyll *a* concentrations, coupled with FT's extreme leakiness, the outer channels could have ''tidally pumped'' phytoplankton biomass into FT at a rate comparable to the rate of local consumption, providing a continuous external supply that maintained the phytoplankton biomass within the lake.

Geometry plus tides disperses phytoplankton.—In addition to providing conduits for importing phytoplankton biomass, the numerous levee breaks around FT also augment dispersion. As the number of openings increases, transport asymmetry is enhanced (e.g., a parcel of water may enter FT through one opening and leave through another), concentration patches become stretched, and the perimeter around a patch (where mixing and dilution operate) is increased. Also, tidal ''jets'' conveying river-derived momentum through the levee breaks increase current velocities within the lake. These processes, as well as the larger wind fetch across FT, probably contributed to enhanced dispersion and to the greater homogeneity (smaller SD and γ_{1500}) of chlorophyll *a* in FT than in MI.

Dispersive transport coupled with spatially variable biological processes could have important general implications. Given the vigorous tidal interaction between FT and adjacent channels, the influence of the local benthic sink probably extends beyond FT: whereas conservative riverine particles may slosh into FT and ultimately slosh out (as in Fig. 5), phytoplankton cells may be permanently removed from the water column by *Corbicula* in the lake and thus prevented from outsloshing (the ''Roach Motel Syndrome'').

Hydrodynamics influences temporal variability of spatial patterns.—Our study captured two timescales of variability for spatial patterns of phytoplankton biomass: tidal (hourly) and neap-spring (weekly). At the tidal timescale, both metrics of spatial variability in MI (SD and γ_{1500}) were larger at high slack than at low slack (Figs. 6 and 8), indicating greater heterogeneity and sharper chlorophyll *a* gradients during the high slack tidal phase. This was probably due to tidal-scale

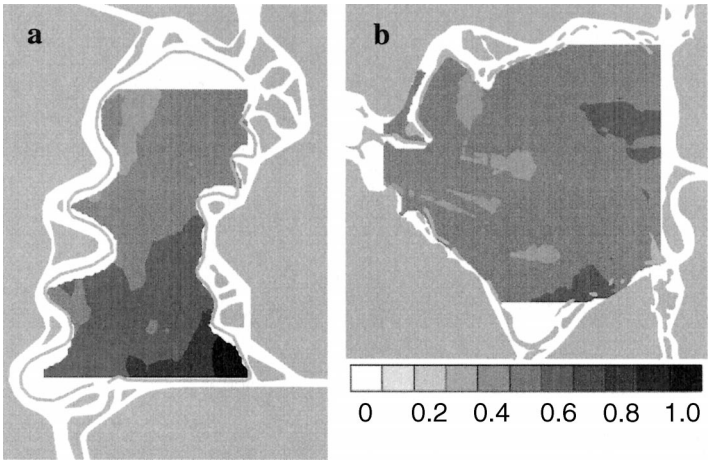

FIG. 10. Contour maps of food-limited potential zooplankton growth rate in (a) Mildred Island and (b) Franks Tract, based on measured distributions of chlorophyll *a* and the empirically derived function between *Daphnia magna* growth rate, G (normalized to the maximum growth rate) and chlorophyll *a* concentration: $G = 1 - \exp[-0.17 \times \text{chl } a - 0.43]$ ($n = 49$, $r^2 = 0.79$; Müller-Solger et al. 2002). The general spatial trends for this tidal phase (neap tide, high slack) are consistent with those of other tidal conditions.

import of low-chlorophyll *a* riverine water during flood tide, similar to the simulated import of particles to MI from the channel during flood (Fig. 3). In FT, a similar process may have occurred, but during ebb instead of flood: SD and γ_{1500} were both larger at low slack than high slack (Figs. 7–8), indicating greater heterogeneity and sharper gradients inside FT during low slack. This could have been caused by import of higher-chlorophyll *a* water from the southeast channels during ebb, similar to the simulated tidal-scale sloshing of numerical particles into FT (Fig. 5). At the weekly timescale, SD and γ_{1500} for both lakes were larger during neap tide than during spring tide, possibly due to weaker currents, shorter tidal excursions, less shear-induced dispersion, and longer residence times during neap tide (Figs. 6–8).

We have shown that phytoplankton biomass can vary substantially within and between shallow tidal habitats and that mechanistic understanding of that time-varying spatial variability requires measurement of the relevant time-varying hydrodynamic and biological processes. What are the implications of that variability for pelagic consumers?

Food available for zooplankton

Our space- and process-intensive study has identified factors that can limit food availability for pelagic secondary productivity. Laboratory assays have shown that growth rate of the cladoceran *Daphnia magna* is a hyperbolic function of chlorophyll *a* concentration in the Sacramento–San Joaquin River Delta (Müller-Solger et al. 2002). With this function we can transform chlorophyll *a* maps into maps of potential zooplankton growth rate (Fig. 10). During our June 1999 study, phytoplankton biomass in both FT and MI was always below that required to support maximum *D. magna* growth. Less-intensive sampling during other months showed similar, food-limiting chlorophyll *a* concentrations and spatial patterns in FT and MI.

This combination of field measurements and laboratory assays suggests that processes regulating phytoplankton biomass distribution (transport, growth, grazing) can also regulate the capacity of shallow habitats to sustain pelagic food webs. Spatial variability in calculated potential *D. magna* growth rate was high within MI during June 1999 (Fig. 10a), with near-maximum growth rates in the high-chlorophyll *a* southeast region and slower growth rates in the low-chlorophyll *a* northern region. Mixing processes within the lake and between the lake and outer channels strongly influenced the food-supply function of this habitat. Localized regions of high chlorophyll *a* and high potential secondary production occurred in MI because it functioned as a producer system (mean $\mu_{\text{eff}}^{\text{zp}} > 0$; Figs. 9c and 10a). Chlorophyll *a* levels in FT were also capable of sustaining zooplankton production (Fig. 10b), even though mean $\mu_{\text{eff}}^{\text{zp}}$ was negative there. This apparent paradox may be explained by tidal pumping of phytoplankton biomass from the outer channels into the lake. Therefore, these habitat types should be viewed as open systems where the pelagic food-supply function can be provided both by hydrodynamic imports as well as internal production.

Zooplankton data for June 1999 (available only for MI) are consistent with the map of potential zooplankton growth rate in Fig. 10a. L. Grimaldo (*personal communication*) obtained densities for individual zooplankton species and life stages in southern and northern MI, which we converted to areal dry mass and to an estimated phytoplankton ingestion rate (Table 5; Kiørboe et al. 1985). Although zooplankton abundance is influenced by numerous factors in addition to food supply (such as predation, migration, and transport), the ~20% north-to-south increase observed for zooplankton areal mass is consistent with the north-to-south increase in observed chlorophyll *a* concentration (Fig. 6) and in calculated potential zooplankton growth rate (Fig. 10a). Estimated total phytoplankton ingestion rates (12–38 mg $C \cdot m^{-2} \cdot d^{-1}$; Table 5) increased southward as well and were an order of magnitude lower

TABLE 5. Zooplankton dry masses (Lehman 2000, Nobriga 1998; J. Orsi, *personal communication*), densities (L. Grimaldo, *personal communication*), and calculated mass per area and phytoplankton ingestion rate (based on empirical relationship by Kiørboe et al. 1985) for southern and northern Mildred Island in June 1999.

Species	Dry mass (μg/individual)	Density (no./m^3)		Mass/area (mg DM/m^2)		Phytoplankton ingestion rate (mg C·m^{-2}·d^{-1})	
		South	North	South	North	South	North
Bosmina longirostris	1.5	342	180	2.4	1.3	0.5	0.1
Cyclopoid copepodids	0.8	293	144	1.1	0.5	0.2	0.0
Cyclops vernalis	5.7	0	36	0.0	1.0	0.0	0.1
Daphnia spp.	5.0	2983	2922	70.1	68.7	14.4	5.2
Diaphanosoma leuchtenbergianum	2.0	244	289	2.3	2.7	0.5	0.2
Eurytemora copepodids	3	293	144	4.1	2.0	0.8	0.2
Eurytemora affinis	6.1	0	253	0.0	7.3	0.0	0.5
Harpacticoid copepods	2.2	0	36	0.0	0.4	0.0	0.0
Other cladocera	2.9	2054	3102	28.0	42.3	5.7	3.2
Other cyclopoid copepods	5.7	0	72	0.0	1.9	0.0	0.1
Other copepod nauplii	0.3	1027	36	1.4	0.1	0.3	0.0
Pseudodiaptomus forbesi	10.6	98	216	4.9	10.8	1.0	0.8
Pseudodiaptomus copepodids	3	4596	1118	64.8	15.8	13.3	1.2
Sinocalanus copepodids	3	147	72	2.1	1.0	0.4	0.1
Sinocalanus doerrii	7.4	147	0	5.1	0.0	1.0	0.0
Total		12 224	8620	186.3	155.8	38.1	11.7

than the mean areal net rate of phytoplankton production for the pelagic food web (225 mg C·m^{-2}·d^{-1}, based on mean $\mu_{\text{eff}}^{\text{zp}}$, phytoplankton biomass, and H). Since the mean zooplankton grazing sink was dwarfed by the net phytoplankton source, zooplankton grazing could not have been a primary force in shaping chlorophyll *a* distributions in MI during June 1999. This situation, where local net *rates* of phytoplankton production exceed zooplankton ingestion rates while *concentrations* of phytoplankton biomass are suboptimal for zooplankton growth, suggests the importance of transport of phytoplankton, predation on zooplankton, and/or species-specific differences in ingestion rates not accounted for here.

Implications for restoration

Lessons for the Sacramento–San Joaquin River Delta and San Francisco Bay.—Results of this study illustrate the importance of expanding our conceptual model beyond the simple notion of generic habitat types. Because of this study's limited temporal scope, we cannot infer that our results represent the function of Mildred Island and Franks Tract during all seasons and years. However, this short-term study does illustrate how functions provided by similar habitats can differ markedly: two seemingly similar open-water habitats can function either as net importers or net suppliers of organic matter to fuel production in pelagic food webs. Moreover, detailed study of processes is essential for revealing the underlying mechanisms that create within-habitat and between-habitat differences in ecosystem functions such as food supply. If a goal of the CALFED San Francisco Bay–Delta Ecosystem Restoration Program is to promote recovery of target species of fishes such as the planktivorous delta smelt, and if the restoration strategy includes creation of new habitats to support pelagic food webs, then it is essential to understand how interactions between physical processes (tidal circulation and mixing) and biological processes (light-limited primary production, competition between benthic and pelagic consumers) shape the outcomes of new habitat formation. Further, it is essential that scientific study and restoration strategies explicitly consider the connectedness of habitats like Franks Tract and Mildred Island to adjacent, and potentially very different, habitats: these are open systems whose ecological functionality relies on tidal transport with neighboring environments as well as on local processes.

An important role for ecosystem science in support of restoration is to identify the mechanisms through which physical–biological interactions constrain the success of meeting restoration goals. Some of these processes can be controlled through physical design of habitats; these include water depth and location and dimensions of levee breaks that determine residence time and circulation pathways. Other processes are, at this point, indeterminate (e.g., the extent of colonization by *Corbicula*) and therefore are primary sources of uncertainty that limit our ability to forecast the specific outcomes of building new habitats. Comparative scientific study of existing habitats prior to the creation of new similar habitats can help reveal the breadth of possible restoration outcomes (i.e., explore restoration uncertainties) and identify processes that can be controlled to optimize the likelihood of meeting restoration goals. Further, critical processes identified by short-term studies like this can be incorporated into studies of variability at longer timescales (seasons, years),

which will be necessary for more complete understanding of these habitats.

Lessons for restoration of other impaired estuaries.—Just as restoration strategies for individual ecosystems should be built from a mechanistic understanding of between-habitat variability, regional or national strategies should include explicit recognition of the variability between ecosystems. No one generic set of restoration actions will be appropriate for all impaired river-estuary systems. The Sacramento–San Joaquin River Delta is an inherently low-productivity ecosystem where multiple stressors have interacted to further depress system productivity in recent decades. For this ecosystem, there is a scientific basis for a restoration plan geared to amplify the supply rate of organic matter to fuel pelagic food webs. This restoration goal is exactly counter to the objectives of restoring estuarine ecosystems impaired by nutrient enrichment, where impairment is manifested as oversupply of organic matter (e.g., Chesapeake Bay; Malone et al. 1999). Although the San Francisco Bay–Delta and Chesapeake Bay have comparable rates of nutrient loading, they function as distinct biogeochemical systems that process those nutrients very differently (Cloern 2001). This contrast illustrates a second role for ecosystem science: to identify and explain the mechanisms of functional variability at the scale of ecosystems. Basic understanding of key ecosystem processes, including those of biogeochemical element cycling, trophic transfers of energy, and hydrodynamics, is essential for designing restoration strategies most appropriate for individual ecosystems.

Acknowledgments

This work was supported by CALFED (Grant #1997-B06), the U.S.G.S. Toxic Substances Hydrology Program, the National Science Foundation, and the Interagency Ecological Program. Many thanks to: our boat captains Jon Yokomizo and Jay Cuetara; Peter Kitinidis and Jean-Marc Guarini for their geostatistical inspiration and expertise; Doug Ball, creator of the RV *Compliance*; data acquisition guru Mike Simpson; water samplers, clam diggers, and sample analyzers Andy Arnsberg, Laurent Chauvaud, Jody Edmunds, Steve Hager, Francis Parchaso, Heather Peterson, Tara Schraga, Bill Sobczak, and Robin Stewart; illustrator Jeanne DiLeo; Robin Stewart for her helpful discussions and October 1998 benthic sample; Lenny Grimaldo for his zooplankton data; and Anke Müller-Solger for her empirical zooplankton growth function. The insightful suggestions of Bill Sobczak, Alan Jassby, Jim Orsi, Michael Kemp, and two anonymous reviewers are greatly appreciated.

Literature Cited

106th U.S. Congress. 2000. Public Law 106-457 (''Estuaries and Clean Waters Act of 2000'').

Alpine, A. E., and J. E. Cloern. 1988. Phytoplankton growth rates in a light-limited environment, San Francisco Bay. Marine Ecology Progress Series **44**:167–173.

APHA (American Public Health Association). 1995. Standard methods for the examination of water and wastewater. Nineteenth edition. APHA, Washington, D.C., USA.

Arar, E. J., and G. B. Collins. 1997. Method 445.0. *In vitro* determination of chlorophyll *a* and pheophytin *a* in marine and freshwater algae by fluorescence. National Exposure Research Laboratory, Office of Research and Development, U.S. Environmental Protection Agency, Cincinnati, Ohio, USA.

Bennett, W. A., and P. B. Moyle. 1996. Where have all the fishes gone? Interactive factors producing fish declines in the Sacramento–San Joaquin Estuary. Pages 519–542 *in* J. T. Hollibaugh, editor. San Francisco Bay: the ecosystem. Pacific Division of the American Association for the Advancement of Science, San Francisco, California, USA.

Butman, C. A., M. Frechette, W. R. Geyer, and V. R. Starczak. 1994. Flume experiments on food supply to the blue mussel, *Mytilus edulis* L., as a function of boundary layer flow. Limnology and Oceanography **39**:1755–1768.

CALFED. 2000*a*. Programmatic record of decision. CALFED Bay–Delta Program, Sacramento, California, USA.

CALFED. 2000*b*. California's water future: a framework for action. CALFED Bay–Delta Program, Sacramento, California, USA.

Casulli, V. 1990*a*. Numerical simulation of shallow water flow. Pages 13–22 *in* G. Gambolati, A. Rinaldo, C. A. Brebbia, and W. G. Gray, editors. Computational methods in surface water hydrology. Springer-Verlag, Berlin, Germany.

Casulli, V. 1990*b*. Semi-implicit finite-difference methods for the two-dimensional shallow water equations. Journal of Computation Physics **86**:56–74.

Casulli, V., and E. Cattani. 1994. Stability, accuracy and efficiency of a semi-implicit method for three-dimensional shallow water flow. Computers and Mathematics with Applications **27**:99–112.

Cheng, R. T., V. Casulli, and J. W. Gartner. 1993. Tidal, residual, intertidal mudflat (TRIM) model and its applications to San Francisco Bay, California. Estuarine, Coastal and Shelf Science **36**:235–280.

Clark, J. S., et al. 2001. Ecological forecasts: an emerging imperative. Science **293**:657–660.

Cloern, J. E. 1982. Does the benthos control phytoplankton biomass in South San Francisco Bay? Marine Ecology Progress Series **9**:191–202.

Cloern, J. E. 1996. Phytoplankton bloom dynamics in coastal ecosystems: a review with some general lessons from sustained investigation of San Francisco Bay, California. Reviews of Geophysics **34**(2):127–168.

Cloern, J. E. 2001. Our evolving conceptual model of the coastal eutrophication problem. Marine Ecology Progress Series **210**:223–253.

Cloern, J. E., C. Grenz, and L. V. Lucas. 1995. An empirical model of the phytoplankton chlorophyll:carbon ratio—the conversion factor between productivity and growth rate. Limnology and Oceanography **40**:1313–1321.

Dame, R. F. 1996. Ecology of marine bivalves. CRC Press, New York, New York, USA.

Dame, R. F., D. Spurrier, and Z. R. G. Zingmark. 1992. *In situ* metabolism of an oyster reef. Journal of Experimental Marine Biology and Ecology **164**:147–159.

Davis, M. A. 2000. ''Restoration''—a misnomer? Science **287**:1203.

Edmunds, J. L., K. M. Kuivila, B. E. Cole, and J. E. Cloern. 1999. Do herbicides impair phytoplankton primary production in the Sacramento–San Joaquin River Delta? Pages 81–87 *in* D. W. Morganwalp and H. T. Buxton, editors. U.S. Geological Survey Water-Resources Investigations Report 99-4018B. U.S. Geological Survey Toxic Substances Hydrology Program, Proceedings of the Technical Meeting 1999. U.S. Geological Survey, West Trenton, New Jersey, USA.

Foe, C., and A. Knight. 1985. The effect of phytoplankton and suspended sediment on the growth of *Corbicula fluminea* (Bivalvia). Hydrobiologia **127**:105–115.

Foe, C., and A. Knight. 1986. A thermal energy budget for

juvenile *Corbicula fluminea*. American Malacological Bulletin, Special Edition **2**:143–150.
Frechette, M., and E. Bourget. 1985. Energy flow between the pelagic and benthic zones: factors controlling particulate organic matter available to an intertidal mussel bed. Canadian Journal of Fisheries and Aquatic Sciences **42**: 1158–1165.
Frechette, M., C. A. Butman, and W. R. Geyer. 1989. The importance of boundary-layer flows in supplying phytoplankton to the benthic suspension feeder, *Mytilus edulis* L. Limnology and Oceanography **34**:19–36.
Gopalan, G., D. A. Culver, L. Wu, and B. K. Trauben. 1998. Effects of recent ecosystem changes on the recruitment of young-of-the-year fish in western Lake Erie. Canadian Journal of Fisheries and Aquatic Science **55**:2472–2479.
Gross, E. S. 1997. Numerical modeling of hydrodynamics and scalar transport in an estuary. Dissertation. Stanford University, Stanford, California, USA.
Gross, E. S., J. R. Koseff, and S. G. Monismith. 1999. Three-dimensional salinity simulations of South San Francisco Bay. Journal of Hydraulic Engineering **125**:1199–1209.
Gunderson, L. H. 1999. Stepping back: assessing for understanding in complex regional systems. Pages 27–40 *in* K. N. Johnson, F. J. Swanson, M. Herring, and S. Greene, editors. Bioregional assessments: science at the crossroads of management and policy. Island Press, Washington, D.C., USA.
Hager, S. W. 1994. Dissolved nutrient and suspended particulate matter data for the San Francisco Bay Estuary, California. October 1991 through November 1993. U.S. Geological Survey Open-File Report 94-471.
Holme, N. A., and A. D. McIntyre. 1971. Methods for the study of marine benthos. IBP handbook number 16. Blackwell Scientific, Oxford, UK.
Hymanson, Z., D. Mayer, and J. Steinbeck. 1994. Long-term trends in benthos abundance and persistence in the upper Sacramento–San Joaquin Estuary. Summary report: 1980–1990. Interagency Ecological Program for the San Francisco Bay/Delta Estuary, Technical Report 38. California Department of Water Resources, Sacramento, California, USA.
Isaaks, E. H., and R. M. Srivastava. 1989. An introduction to applied geostatistics. Oxford University Press, New York, New York, USA.
Jassby, A. D., and J. E. Cloern. 2000. Organic matter sources and rehabilitation of the Sacramento–San Joaquin Delta (California, USA). Aquatic Conservation: Marine and Freshwater Ecosystems **10**:323–352.
Jassby, A. D., J. E. Cloern, and B. E. Cole. 2002. Annual primary production: patterns and mechanisms of change in a nutrient-rich tidal ecosystem. Limnology and Oceanography **47**:698–712.
Jones, M. L. 1999. Great Lakes-St. Lawrence River Basin assessments: science review. Pages 153–156 *in* K. N. Johnson, F. J. Swanson, M. Herring, and S. Greene, editors. Bioregional assessments: science at the crossroads of management and policy. Island Press, Washington, D.C., USA.
Kimmerer, W. J., and J. J. Orsi. 1996. Changes in the zooplankton of the San Francisco Bay Estuary since the introduction of the clam *Potamocorbula amurensis*. Pages 403–424 *in* J. T. Hollibaugh, editor. San Francisco Bay: the ecosystem. Pacific Division of the American Association for the Advancement of Science, San Francisco, California, USA.
Kiørboe, T., F. Møhlenberg, and K. Hamburger. 1985. Bioenergetics of the planktonic copepod *Acartia tonsa*: relation between feeding, egg production and respiration, and composition of specific dynamic action. Marine Ecology Progress Series **26**:85–97.
Kitinidis, P. K. 1997. Introduction to geostatistics: applications in hydrogeology. Cambridge University Press, Cambridge, UK.
Koseff, J. R., J. K. Holen, S. G. Monismith, and J. E. Cloern. 1993. Coupled effects of vertical mixing and benthic grazing on phytoplankton populations in shallow, turbid estuaries. Journal of Marine Research **51**:843–868.
Kurth, R., and M. Nobriga. 2001. Food habits of larval splittail. Interagency Ecological Program Newsletter **14**:40–41.
Lauritsen, D. D. 1986. Filter-feeding in *Corbicula fluminea* and its effect on seston removal. Journal of the North America Benthological Society **5**:165–172.
Lehman, P. W. 2000. Phytoplankton biomass, cell diameter, and species composition in the low salinity zone of northern San Franciso Bay Estuary. Estuaries **23**:216–230.
Lucas, L. V., J. E. Cloern, J. R. Koseff, S. G. Monismith, and J. K. Thompson. 1998. Does the Sverdrup critical depth model explain bloom dynamics in estuaries? Journal of Marine Research **56**:375–415.
Lucas, L. V., J. R. Koseff, J. E. Cloern, S. G. Monismith, and J. K. Thompson. 1999*a*. Processes governing phytoplankton blooms in estuaries. I: the local production-loss balance. Marine Ecology Progress Series **187**:1–15.
Lucas, L. V., J. R. Koseff, S. G. Monismith, J. E. Cloern, and J. K. Thompson. 1999*b*. Processes governing phytoplankton blooms in estuaries. II: the role of horizontal transport. Marine Ecology Progress Series **187**:17–30.
Lucas, L. V., and J. E. Cloern. 2002. Effects of tidal shallowing and deepening on phytoplankton production dynamics: a modeling study. Estuaries, *in press*.
Malone, T. C., A. Malej, L. W. Harding, Jr., N. Smodlaka, and R. E. Turner, editors. 1999. Ecosystems at the land-sea margin. Drainage basin to coastal sea. American Geophysical Union, Washington, D.C., USA.
McMahon, R. F. 1991. Mollusca: Bivalvia. Pages 315–399 *in* J. H. Thorp and A. P. Covich, editors. Ecology and classification of North American freshwater invertebrates. Academic Press, San Diego, California, USA.
McMahon, R. F. 1999. Invasive characteristics of the freshwater bivalve *Corbicula fluminea*. Pages 315–343 *in* R. Claudi and J. H. Leach, editors. Nonindigenous freshwater organisms: vectors, biology, and impacts. Lewis, Boca Raton, Florida, USA.
Monsen, N. 2001. A study of subtidal transport in Suisun Bay and the Sacramento–San Joaquin Delta, California. Dissertation. Stanford University, Stanford, California, USA.
Müller-Solger, A. B., A. D. Jassby, and D. C. Müller-Navarra. 2002. Nutritional quality of food resources for zooplankton (*Daphnia*) in a tidal freshwater system (Sacramento–San Joaquin River Delta, USA). Limnology and Oceanography, *in press*.
Newell, C. F., and S. E. Shumway. 1993. Grazing of natural particulates by bivalve mollusks: a spatial and temporal perspective. Pages 85–148 *in* R. F. Dame, editor. Bivalve filter feeders. Springer-Verlag, Berlin, Germany.
Nobriga, M. N. 1998. Trends in the food habits of larval delta smelt, *Hypomesus transpacificus*, in the Sacramento–San Joaquin Estuary. Thesis. California State University, Sacramento, California, USA.
O'Riordan, C. A., S. G. Monismith, and J. R. Koseff. 1995. The effect of bivalve excurrent jet dynamics on mass transfer in a benthic boundary layer. Limnology and Oceanography **40**:330–344.
Platt, T., D. F. Bird, and S. Sathyendranath. 1991. Critical depth and marine primary production. Proceedings of the Royal Society of London, Series B, Biological Sciences **246**:205–218.
Reiners, W. A., and K. L. Driese. 2001. The propagation of ecological influences through heterogeneous environmental space. BioScience **51**:939–950.

Robertson, G. P. 1998. GS+: Geostatistics for the environmental sciences. Gamma Design Software, Plainwell, Michigan, USA.
San Francisco Estuary Project. 2001. Supply: islands of water. Estuary **10**(2):3.
Schrope, M. 2001. Save our swamp. Nature **409**:128–130.
Thomas, J. W. 1999. Learning from the past and moving to the future. Pages 11–25 *in* K. N. Johnson, F. J. Swanson, M. Herring, and S. Greene, editors. Bioregional assessments: science at the crossroads of management and policy. Island Press, Washington, D.C., USA.
Thompson, J. K. 1999. The effect of infaunal bivalve grazing on phytoplankton bloom development in South San Francisco Bay. Dissertation. Stanford University, Stanford, California, USA.
Wildish, D. J., and D. D. Kristmanson. 1984. Importance to mussels of the benthic boundary layer. Canadian Journal of Fisheries and Aquatic Science **41**:1618–1625.
Winternitz, L. H. 1992. Estimating secondary production levels of the Asiatic clam *Corbicula fluminea* from the Sacramento–San Joaquin Estuary. Thesis. University of San Francisco, San Francisco, California, USA.
Zedler, J. B., editor. 2001. Handbook for restoring tidal wetlands. CRC Press, Boca Raton, Florida, USA.

APPENDIX

An appendix containing animations in the form of MPG movies of the three numerical simulations illustrated in Figs. 3–5 is available in ESA's Electronic Data Archive: *Ecological Archives* A012-015-A1.